Published in final edited form as:
Cancer Cell. 2010 January 19; 17(1): 53. doi:10.1016/j.ccr.2009.11.021.

IAP REGULATION OF METASTASIS

Swarna Mehrotra,
Prostate Cancer Discovery and Development Program, University of Massachusetts Medical School, Worcester, MA 01605

Lucia R. Languino,
Prostate Cancer Discovery and Development Program, University of Massachusetts Medical School, Worcester, MA 01605

Christopher M. Raskett,
Prostate Cancer Discovery and Development Program, University of Massachusetts Medical School, Worcester, MA 01605

Arthur M. Mercurio,
Department of Cancer Biology, University of Massachusetts Medical School, Worcester, MA 01605

Takehiko Dohi*, and
Prostate Cancer Discovery and Development Program, University of Massachusetts Medical School, Worcester, MA 01605

Dario C. Altieri*
Prostate Cancer Discovery and Development Program, University of Massachusetts Medical School, Worcester, MA 01605

SUMMARY

Inhibitor-of-Apoptosis (IAP) proteins contribute to tumor progression, but the requirements of this pathway are not understood. Here, we show that intermolecular cooperation between XIAP and survivin stimulates tumor cell invasion and promotes metastasis. This pathway is independent of IAP inhibition of cell death. Instead, a survivin-XIAP complex activates NFκB, which in turn leads to increased fibronectin gene expression, signaling by β1 integrin(s), and activation of cell motility

Correspondence: Dario C. Altieri, M.D., Department of Cancer Biology, LRB428, University of Massachusetts Medical School, 364 Plantation Street, Worcester, MA 01605, Tel. (508) 856-5775; FAX (508) 856-5792; dario.altieri@umassmed.edu.
*These authors contributed equally to this work.

SIGNIFICANCE

Metastasis is a hallmark of tumor progression, characterized by the dissemination of cancer cells to distant organs. Despite a better understanding of this process, often characterized by deregulated gene expression, anti-metastatic therapies do not presently exist, and patients with disseminated disease have limited options. We now show that Inhibitor-of-Apoptosis (IAP) molecules function as direct activators of tumor cell motility and metastasis genes independently of their roles in cytoprotection. IAP antagonists are now being tested in early phase clinical trials, and these agents may provide first-in-class anti-metastatic therapies in cancer patients.

SUPPLEMENTAL INFORMATION

Supplemental material (Supplemental Data, Experimental Procedures, and References) accompanies this paper.

ACCESSION NUMBERS

The analysis of microarray datasets is available at miamexpress@ebi.ac.uk under accession number E-MEXP-2184.

CONFLICT OF INTEREST

The authors declare that they have no competing interest.

kinases, FAK and Src. Therefore, IAPs are direct metastasis genes, and their antagonists could provide anti-metastatic therapies in cancer patients.

Keywords

Inhibitor of apoptosis; survivin; XIAP; fibronectin; metastasis; NFκB

INTRODUCTION

The dissemination of tumor cells to distant organs, i.e. metastasis (Nguyen and Massague, 2007), heralds a nearly invariably fatal phase of epithelial malignancies, with few, if any, therapeutic options. This process reflects the acquisition of multiple molecular traits by tumor cells, including the ability to counteract the cell death program initiated by detachment from the extracellular matrix, or anoikis (Frisch and Screaton, 2001), proteolyze and migrate through basement membrane(s), invade blood or lymphatic vessels, and proliferate in unrelated microenvironments (Weigelt et al., 2005). The exact timing of these processes is unknown, and whether they reflect sequential adaptive changes (Scheel et al., 2007), or selection of specially endowed clones (Talmadge, 2007), has been debated. However, one invariable feature of the metastatic process is deregulated gene expression, which affects sequential stages of tumor cell invasion, organ tropism, and growth at distant sites (Nguyen and Massague, 2007). A potential loss of 'metastasis-suppressor' genes may also contribute to this pathway (Stupack et al., 2006).

Although the molecular requirements of metastasis remain largely elusive, 'outside-in' signaling initiated by ligation of integrin cell surface receptors (Ginsberg et al., 2005) with extracellular matrix proteins (Juliano et al., 2004), likely plays a pivotal role in this process. As an abundant constituents of the extracellular matrix, fibronectin binds multiple integrins (Cukierman et al., 2002), resulting in the activation of Focal Adhesion Kinase (FAK) (Sieg et al., 2000), Src (Yeatman, 2004), Akt (Irie et al., 2005), as well as modulation of small GTPases of the Rho family (Nobes and Hall, 1995). In response to these signals, cells remodel their actin cytoskeleton (Juliano et al., 2004), express matrix metalloproteinases (Han et al., 2006), become migratory (Livant et al., 2000), invade basement membranes (Gaggioli et al., 2007), and acquire the ability to resist apoptosis (Fornaro et al., 2003).

In this context, aberrantly increased cell survival is an invariable requirement of metastasis (Mehlen and Puisieux, 2006), and is typically contributed via deregulated expression of Bcl-2 (Cory and Adams, 2002) or Inhibitor-of-Apoptosis (IAP) (Srinivasula and Ashwell, 2008) cytoprotective proteins. However, some of these molecules, especially IAPs, have recently emerged as broader regulators of cellular homeostasis, with functions extending beyond apoptosis inhibition (Srinivasula and Ashwell, 2008). For instance, IAP family protein XIAP has been linked to the activation of multiple gene expression networks, including Smad/TGFβ (Birkey Reffey et al., 2001), JNK (Sanna et al., 1998), or NFκB (Hofer-Warbinek et al., 2000; Lu et al., 2007), whereas survivin plays essential roles in mitosis, the cellular stress response, and developmental pathways of gene expression (Altieri, 2008). How these multiple functions of IAPs work together in cellular homeostasis is unclear, and the exact contribution of these non-cytoprotective mechanisms, if any, to tumor progression has not been investigated.

In this study, we asked whether IAP signaling affected metastasis as a key determinant of unfavorable disease outcome.

RESULTS

IAP-mediated tumor cell invasion

To begin investigating a role of IAPs in tumor progression, we first silenced the expression of XIAP or survivin in invasive breast adenocarcinoma MDA-MB-231 (Figure 1A), or prostate adenocarcinoma PC3 (Figure 1B) cells. Transfection of these cells with XIAP- or survivin-directed small interfering RNA (siRNA) suppressed the expression of the intended IAP protein, but not vice versa, whereas a non-targeting siRNA had no effect (Figure 1A, B). Under these conditions, survivin or XIAP knockdown inhibited MDA-MB-231 or PC3 cell invasion through Matrigel inserts, as compared with control transfectants (Figure 1C, D). Similar results were obtained with siRNA silencing of these IAPs in colorectal adenocarcinoma HCT116 cells, whereas a non-targeting siRNA had no effect (Figure 1E). In addition, siRNA knockdown of a different IAP, cIAP1, also abolished Matrigel invasion of PC3 cells (Figure 1F), suggesting that tumor cell invasion was a general property of multiple IAPs.

Next, we examined the specificity of this pathway, and we used clones of non-invasive breast adenocarcinoma MCF-7 cells stably transfected with survivin. These cells, designated MCF-7 SVV, express a 2- to 3-fold increased survivin levels compared to MCF-7 cells (Figure S1A), thus similar to more invasive cell types (Figure 1A). Compared to parental cultures, MCF-7 SVV cells did not exhibit changes in cell proliferation (Figure S1B), adhesion to fibronectin- or collagen-containing substrates (Figure S1C), remodeling of the actin cytoskeleton (Figure S1D), or expression of various integrins (Figure S1E). Instead, MCF-7 SVV cells became highly migratory on collagen-coated inserts, compared to parental cultures (Figure S1F), or MCF-7 cells transfected with empty plasmid (not shown). Consistent with this, two independent clones of MCF-7 SVV cells showed markedly enhanced invasion through Matrigel-coated inserts, whereas non-transfected MCF-7 cells were not invasive (Figure 1G).

Confirming the specificity of IAPs in this response, siRNA knockdown of XIAP or survivin in MCF-7 SVV cells (Figure 2A) suppressed Matrigel invasion, whereas a non-targeting siRNA had no effect (Figure 2B). Conversely, cell viability was only minimally affected after XIAP (7%) or survivin (14.2%) silencing, compared to control transfectants (4.8%). cIAP1 knockdown also reduced Matrigel invasion of MCF-7 SVV cells from 61.5±11.1 (control siRNA) to 11.3±1.6 invaded cells per field (p=0.0003, n=10). As an independent approach, we transduced MCF-7 SVV cells with an adenovirus (pAd) encoding a dominant negative survivin Cys84Ala/Thr34Ala mutant (pAd-T34A/C84A). Although expressed at comparable levels as pAd-GFP by fluorescence microscopy (Figure 2C, *top*), this survivin mutant abolished Matrigel invasion (Figure 2C), whereas cell cycle kinetics or cell viability were not affected within the same time interval (Figure S2A). Finally, we stably silenced the expression of XIAP in MCF-7 SVV cells using a lentivirus construct encoding XIAP-directed short hairpin RNA (Figure 2D). Independently established clones of these cells, designated MCF-7 SVV-XIAP KD, showed marked inhibition of Matrigel invasion, as compared with control cultures (Figure 2E).

To independently validate these findings, we next examined a second tumor model, HCT116 cells, in which siRNA silencing of XIAP or survivin suppressed Matrigel invasion (Figure 1E). Consistent with this, homozygous deletion of XIAP ($XIAP^{-/-}$) in HCT116 cells (Figure 2F) completely abolished tumor cell invasion, whereas wild type HCT116 cells ($XIAP^{+/+}$) were highly invasive (Figure 2G).

IAP anti-apoptotic functions are not required for tumor cell invasion

To test whether IAP cytoprotection contributed to tumor cell invasion, we next used a model of rat insulinoma INS-1 cells. Previous studies showed that stable transfection of survivin in

these cells (INS-1 SVV) (Figure S2B) does not inhibit apoptosis, due to lack of mitochondrial import (Dohi et al., 2007). INS-1 SVV cells readily invaded through Matrigel inserts whereas control INS-1 transfectants were not invasive (Figure S2C). In addition, stable transfection of anti-apoptotic Bcl-2 in INS-1 cells (Figure S2B), which promoted exponential tumor growth in vivo (Dohi et al., 2007), did not mediate tumor cell invasion (Figure S2C). We next asked whether a similar paradigm applied to XIAP, and we stably transfected $XIAP^{-/-}$ HCT116 cells with an Asp143Ala/Trp310Ala XIAP double mutant (D143A/W310A) that does not bind caspase 3 (D143A mutation) or caspase 9 (W310A mutation), and is thus devoid of anti-apoptotic functions (Lewis et al., 2004) (Figure 2H). Independent clones of this cell line robustly invaded through Matrigel inserts, quantitatively indistinguishably from $XIAP^{-/-}$ cells reconstituted with wild type, i.e. anti-apoptotic, XIAP (Figure 2I).

IAP induction of fibronectin regulates tumor cell invasion

To begin understanding how IAPs promote tumor cell invasion, we next looked at the gene expression profile of model MCF-7 SVV cells, in which expression of survivin, alone, was sufficient to confer an invasive phenotype (Figure 1F). Microarray analysis of these cells revealed a significant upregulation of multiple extracellular matrix proteins implicated in cell invasion, including lumican (4106-fold), fibronectin (334-fold), and laminin α4 (105-fold). Accordingly, MCF-7 SVV cells exhibited a >120-fold upregulation of fibronectin mRNA, by real-time PCR (Figure 3A), and increased fibronectin promoter activity, by luciferase reporter assay (Figure 3B), compared to parental MCF-7 cells. Collagen type 1 α1 and collagen type 5 α2 mRNAs were also increased in MCF-7 SVV cells, albeit less prominently, whereas expression of laminin 5 was not significantly different, compared to parental cultures (Figure 3A). Consistent with these data, MCF-7 SVV cells exhibited dramatically increased endogenous fibronectin protein content, by fluorescence microscopy (not shown), and Western blotting (Figure 3C). This newly produced fibronectin was released in the conditioned medium of MCF-7 SVV cells (Figure 3D), and was sufficient to support tumor cell migration on Transwell inserts in the absence of exogenous substrate (Figure 3E). In contrast, parental MCF-7 cells did not migrate in the absence of substrate (Figure 3E). Similar results were obtained with an unrelated cell type, as INS-1 cells stably transfected with survivin (INS-1 SVV) also exhibited a 7- to 8-fold increased fibronectin mRNA (Figure S3A), and protein (Figure S3B). In contrast, INS-1 Bcl-2 transfectants, or cells transfected with a control plasmid, showed no modulation of fibronectin levels (Figure S3A, B).

Using breast cancer as a model, we next asked whether a relationship between IAP and fibronectin expression existed in human tumors. Analysis of two independent patient cohorts revealed that survivin and fibronectin were coordinately increased in tumor *versus* normal tissues (Figure 3F). Similarly, invasive breast adenocarcinoma cell lines SUM159 and HBL100 contained high levels of endogenous fibronectin (Figure S3C), suggesting that its expression segregated with the tumor cell population, rather than stromal cells.

Finally, we tested whether fibronectin produced and released by IAP-expressing cells contributed to tumor cell invasion. Here, siRNA knockdown of fibronectin in MCF-7 SVV cells (Figure 3G) significantly inhibited Matrigel invasion, as compared with control transfectants (Figure 3H). Similarly, preincubation of MCF-7 SVV cells with a function-blocking antibody to β1 integrin(s), which comprise the main fibronectin receptor on these cells, abolished tumor cell invasion, whereas non-binding IgG was ineffective (Figure 3I).

IAP intermolecular cooperation activates NFκB

We next asked how IAP may transcriptionally upregulate fibronectin, and we focused on a potential role of NFκB in this response. For these experiments, we stably transfected survivin in wild type (WT) or $XIAP^{-/-}$ mouse embryonic fibroblasts (MEF) that have very low levels

of endogenous survivin (Figure S4A). Expression of survivin in $XIAP^{+/+}$ cells (clones #44 and #68) resulted in nuclear translocation of p65 NFκB (Figure 4A), and increased NFκB promoter activity, quantitatively similar to TNFα stimulation (Figure 4B). In contrast, survivin expression in $XIAP^{-/-}$ cells (clones #2 and #5) had no effect on NFκB translocation (Figure 4A), or NFκB promoter activity (Figure 4B). By EMSA, a radiolabeled NFκB probe bound to nuclear extracts in $XIAP^{+/+}$ cells transfected with survivin, which was supershifted by an antibody to p65 NFκB, but not IgG (Figure 4C). Conversely, expression of survivin in a $XIAP^{-/-}$ background had minimal effect on NFκB-protein complexes (Figure 4C). In 'add back' experiments, transfection of survivin-expressing $XIAP^{-/-}$ cells with wild type XIAP restored the formation of NFκB complexes, whereas a RING-less XIAP mutant (RING-Δ) was ineffective (Figure 4C). Similarly, INS-1 cells stably transfected with a survivin S20A mutant, which constitutively binds XIAP (Dohi et al., 2007), strongly activated NFκB promoter activity, with or without TNFα (Figure 4D). In contrast, INS-1 cells expressing a survivin S20E mutant that does not bind XIAP (Dohi et al., 2007), showed no NFκB promoter activity (Figure 4D). Finally, siRNA knockdown of survivin in MCF-7 SVV cells significantly reduced NFκB promoter activity, compared to control transfectants (Figure S4B). Therefore, a survivin-XIAP complex (Dohi et al., 2007) activates NFκB.

As far as the mechanism(s) of NFκB activation under these conditions, addition of recombinant XIAP to MCF-7 cell extracts promoted the phosphorylation of the negative NFκB regulator, IκBα (Figure 4E). However, the combination of survivin plus XIAP further enhanced IκBα phosphorylation (Figure 4E), in a reaction stabilized by the proteasome inhibitor, lactacystin (Figure S3C). Conversely, a Val80Asp (V80D) XIAP mutant that does not activate NFκB (Lu et al., 2007), had no effect on IκBα phosphorylation, with or without lactacystin (Figure S4C). Accordingly, reconstitution of $XIAP^{-/-}$ cells with wild type XIAP, but not V80D XIAP mutant, stimulated NFκB promoter activity with and without TNFα (Figure S4D).

NFκB-induction of fibronectin contributes to IAP-mediated tumor cell invasion

Consistent with a bona fide NFκB target gene, TNFα stimulation of MCF-7 or MCF-7 SVV cells resulted in increased fibronectin expression, albeit more prominently in survivin transfectants (Figure 4F). Conversely, siRNA knockdown of p65 NFκB (Figure S4E) suppressed endogenous fibronectin expression in MCF-7 SVV cells, as compared with control siRNA (Figure 4G). Similarly, siRNA silencing of survivin or XIAP also comparably suppressed fibronectin expression in MCF-7 SVV cells (Figure 4H). Functionally, siRNA knockdown of p65 NFκB (Figure S4E), or expression of a phosphorylation-defective IκBα 'super-repressor' mutant (Figure S4F), inhibited Matrigel invasion of MCF-7 SVV cells, as compared with control transfectants (Figure 4I).

Signaling requirements of IAP-mediated tumor cell invasion

To identify downstream effectors of IAP-directed tumor cell invasion, we next focused on kinase cascades implicated in cell motility. When attached to substrate, MCF-7 SVV cells exhibited constitutive phosphorylation of FAK on Tyr397 (Figure 5A), and Src on Tyr418 (Figure 5B), compared to parental MCF-7 cells. In contrast, phosphorylated Akt (Figure 5C), or ERK1,2 (Figure 5D) was comparable in the two cell types, and total kinase protein content was unchanged (Figure 5A–D). Stable knockdown of XIAP in MCF-7 SVV cells (MCF-7 SVV-XIAP KD) abolished FAK and Src phosphorylation, and significantly reduced endogenous fibronectin content in these cells (Figure 5E), reinforcing a role of IAP intermolecular cooperation in this response. Similarly, Src was constitutively phosphorylated in INS-1 cells expressing wild type survivin, but not a survivin S20E mutant (Figure 5F) that does not bind XIAP (Dohi et al., 2007).

Functionally, targeting FAK with a truncated dominant negative FAK protein, FRNK (Figure S5A), inhibited MCF-7 SVV cell invasion through Matrigel (Figure 5G). Similarly, two unrelated pharmacologic antagonists of Src, PP2 (Figure 5H), or SU6656 (Figure 5I), suppressed Matrigel invasion of MCF-7 SVV (Figure 5H, I), or MDA-MB-231 (Figure S5B) cells, without affecting cell viability or cell cycle kinetics (Figure 5J). In contrast, pharmacologic antagonists of MEK (PD98059 or U0126), or PI3 kinase (LY294002) had no effect on IAP-mediated tumor cell invasion (Figure 5H). Confirming their activity, all inhibitors abolished the phosphorylation of their intended target kinase (Figure S5C).

IAP protection from anoikis

The ability of tumor cells to remain viable when detached from the extracellular matrix may contribute to metastasis, and a role of IAP in this response was next investigated. MCF-7 cells forced to remain in suspension showed time-dependent anoikis (Figure 6A), and release of apoptogenic Smac from mitochondria (Figure 6B). In contrast, MCF-7 SVV cells were protected from anoikis (Figure 6A), and exhibited reduced release of Smac from mitochondria (Figure 6B). When attached to substrate, no differences were observed in background levels of Smac release between MCF-7 and MCF-7 SVV cells (Figure 6B). Survivin silencing by siRNA reversed cytoprotection of MCF-7 SVV cells in suspension (Figure S6), and strongly enhanced anoikis (Figure 6B). Conversely, survivin knockdown in attached MCF-7 SVV cells (Figure S6) did not significantly reduce cell viability within the same time interval (Figure 6C).

Although survivin inhibited anoikis (Figure 6C), MCF-7 and MCF-7 SVV cells grew comparably as colonies in soft agar (Figure 6D), and MCF-7 SVV cells in suspension did not release survivin from mitochondria into the cytosol (Figure 6E), which is required for cytoprotection (Dohi et al., 2007). Instead, MCF-7 SVV cells in suspension, but not parental MCF-7 cells, exhibited constitutive phosphorylation of FAK and Src (Figure 6F), which has been implicated in protection from anoikis (Bouchard et al., 2008). In addition, siRNA knockdown of fibronectin (Figure 6G), or its receptor, β1 integrin(s) (Figure 6H), suppressed FAK and Src phosphorylation in MCF-7 SVV cells in suspension.

IAP-dependent metastasis

For these studies, we used a liver metastasis model, in which tumor cells are injected directly into the spleen of immunocompromised SCID/beige mice, followed by splenectomy after 24 h to avoid potential interference of primary tumor growth on liver metastasis. Splenic injection of MCF-7 cells did not result in significant liver metastasis (Figure 7A, Figure S7A), and organs in this group were histologically normal (Figure 7B). In contrast, MCF-7 SVV cells reconstituted in the same model gave rise to extensive metastatic localization of the liver (Figure 7A, Figure S7A), with foci of viable epithelial cells in the liver parenchyma (Figure 7B, Figure S7B). Liver metastases of MCF-7 SVV cells stained for phosphorylated FAK (Figure S7C) consistent with a potential role of activated FAK in this pathway, in vivo. In contrast, stable knockdown of XIAP in MCF-7 SVV cells (MCF-7 SVV-XIAP KD) completely suppressed their ability to metastasize to the liver (Figure 7A, Figure S7A).

As an independent tumor model, intrasplenic injection of wild type $XIAP^{+/+}$ HCT116 cells resulted in massive metastatic colonization of the liver, with nearly complete substitution of the hepatic parenchyma by the tumor cell population (Figure 7C). In contrast, $XIAP^{-/-}$ cells did not significantly metastasize to the liver (Figure 7C). Quantification of liver metastasis revealed that HCT116 cells expressing wild type XIAP produced a >2-fold increase in liver weight, as compared with non-injected animals or mice reconstituted with $XIAP^{-/-}$ cells (Figure S7D).

We have shown above that IAP cytoprotection is not required for tumor cell invasion, in vitro, and we next asked whether a similar paradigm applied to metastatic dissemination, in vivo. XIAP$^{-/-}$ HCT116 cells stably transfected with D143A/W310A XIAP double mutant devoid of anti-apoptotic function (Lewis et al., 2004), produced extensive liver metastasis (p=0.038 compared to normal liver, Figure S7D), quantitatively indistinguishable from XIAP$^{+/+}$ HCT116 cells (Figure 7C; not significant, Figure S7D). Similarly, INS-1 clones stably transfected with wild type survivin, which is not cytoprotective in these cells (Dohi et al., 2007), gave rise to systemic disease in SCID/beige mice, as judged by time-dependent decrease in blood glucose (Figure 7D), a biomarker of aberrant insulin production by insulinoma cells. This was associated with prominent metastatic dissemination of insulin-producing INS-1 cells to the liver (Figure 7E, F). In contrast, animals injected with INS-1 cells expressing anti-apoptotic Bcl-2 did not show changes in blood glucose levels (Figure 7D), and generated negligible liver metastasis (Figure 7F, Figure S7E). Previously, these cells promoted exponential growth of superficial tumors in SCID/beige mice, validating the activity of Bcl-2 (Dohi et al., 2007).

DISCUSSION

In this study, we have shown that intermolecular cooperation between IAP proteins, XIAP and survivin, promotes tumor cell invasion in vitro and metastatic dissemination in vivo. This pathway is independent of the role of IAPs in cell survival. Instead, these molecules orchestrate a cellular network in disparate tumor cell types centered on NFκB activation, transcriptional upregulation of fibronectin, autocrine/paracrine signaling by β1 integrins, and constitutive phosphorylation, i.e. activation, of cell motility kinases, FAK and Src (Figure 8). These data identify IAPs as direct metastasis genes, opening prospects for therapeutic intervention against these targets in patients with advanced and disseminated disease.

Beyond their roles in cytoprotection, it is now clear that IAPs function as broader regulators of cellular homeostasis, intercalated in cell division, metabolism and activation of multiple intracellular signaling pathways, including NFκB, TGFβ or JNK (Srinivasula and Ashwell, 2008). The data presented here position IAP signaling in the control of multiple, independent stages of the metastatic cascade conferring a general motility phenotype to tumor cells, unaffected by substrate attachment, competent to withstand anoikis, and ideal to support colonization of distant organs (Figure 8). In this context, a role of IAPs in cell motility may be evolutionary conserved, as a *Drosophila* IAP homolog has been implicated in cytoskeletal rearrangement and cell migration (Geisbrecht and Montell, 2004), via activation of small GTPase signaling (Oshima et al., 2006). However, whether a similar paradigm extended to mammalian cells, especially tumor cells, has been controversial, and a recent report suggested that silencing of IAPs actually increased tumor cell motility, potentially through enhanced c-Raf stability (Dogan et al., 2008). It is possible that the discrepancy between these results (Dogan et al., 2008) and the data presented here may reflect context-specific utilization of activated c-Raf for cell motility, as opposed to cell invasion. On the other hand, c-Raf has been known to inhibit (Slack et al., 1999), rather than promote (Dogan et al., 2008) cell migration, potentially by suppressing integrin activation (Hughes et al., 1997).

Here, the upstream step in IAP-mediated metastasis involved activation of NFκB-dependent gene expression. A link between IAPs, mostly XIAP, and NFκB activity (Srinivasula and Ashwell, 2008) has been previously associated with ubiquitination by RING-associated XIAP E3 ligase (Lewis et al., 2004), Smad4 signaling (Birkey Reffey et al., 2001), negative modulation by XIAP-binding protein(s) (Resch et al., 2009), or phosphorylation-induced degradation of IκBα, at least in endothelial cells (Hofer-Warbinek et al., 2000). Here, reconstitution experiments in XIAP$^{-/-}$ cells, together with ‘add-back’ studies using wild type or mutant recombinant proteins, demonstrated that NFκB activation requires the assembly of

a survivin-XIAP intermolecular complex. Structurally, this may favor the recruitment of the adapter protein, TAB1 (Lu et al., 2007), resulting in downstream activation of the IKK kinase, TAK1, and IκBα phosphorylation (Hofer-Warbinek et al., 2000). Accordingly, a V80D XIAP mutant defective in TAB1 binding (Lu et al., 2007) did not cooperate with survivin in NFκB activation. However, additional requirements of a survivin-XIAP complex likely contribute to this response, as RING-less XIAP, or a Lys467Ala XIAP mutant that abolishes E3 ligase activity also failed to synergize with survivin in stimulating NFκB (T.D. and D.C.A., unpublished observations), in agreement with previous findings (Lewis et al., 2004). Broadly, IAP heterodimerization may function as general mechanism of cellular homeostasis (Srinivasula and Ashwell, 2008), as a survivin-BRUCE complex may regulate cytokinesis (Pohl and Jentsch, 2008), and a survivin-XIAP interaction (Dohi et al., 2007) opposes tumor cell apoptosis, by enhancing XIAP stability and synergistically inhibiting caspase(s) (Dohi et al., 2004).

Previously, a link between NFκB activity and metastasis has been tied to stimulation of epithelial-mesenchymal transition (EMT), expression of matrix metalloproteinase-9 (MMP-9), or repression of putative metastasis-suppressor genes (Naugler and Karin, 2008). Here, IAP activation of NFκB did not result in morphological features of EMT, as judged by the unchanged levels of E-cadherin or MMP-2 or -9 (S.M. and D.C.A., unpublished observations). Conversely, NFκB activity under these conditions contributed to a broad ‘adhesion gene signature’ in tumor cells, characterized by a several hundred fold upregulation of fibronectin. There is evidence that this pathway may occur during tumor progression in vivo, as transgenic mice expressing survivin in the urinary bladder exhibited a similar ‘adhesion gene signature’, linked to aggressive tumor behavior and abbreviated survival (Salz et al., 2005). Correlative observations in humans seem consistent with this scenario, as fibronectin is over-expressed in various epithelial malignancies (Bittner et al., 2000), and linked to disease dissemination (Clark et al., 2000), and shortened overall and disease-free survival (Yao et al., 2007). Several mechanistic models have been proposed to explain these findings, and elevated levels of fibronectin have been linked to loss of epithelial polarity (Nelson and Bissell, 2006), increased tissue rigidity (Paszek et al., 2005), disruption of mammary acinar morphogenesis (Williams et al., 2008), resistance to hormonal therapy (Helleman et al., 2008), and formation of a metastatic niche (Kaplan et al., 2005).

The data presented here suggest a broader scenario, establishing fibronectin as a direct mediator of tumor cell invasion. This process is postulated to involve a paracrine/autocrine signaling circuitry (Figure 8), in which fibronectin over-produced and released extracellularly by IAP-expressing tumor cells binds back to the cell surface, engaging cognate β1 integrins, and triggering cell- and matrix-autonomous activation of cell motility kinases, FAK and Src (Figure 8). Accordingly, outside-in signaling mediated by β1 integrins (Ginsberg et al., 2005), leads to phosphorylation of Src (Mitra and Schlaepfer, 2006), FAK (Sieg et al., 2000), and mediates tumor cell invasion, in vivo (Parsons et al., 2008). Although antibody inhibition studies demonstrated that β1 integrins are essential for IAP-mediated tumor cell invasion, immunologic or molecular targeting of fibronectin was only partially, i.e. 50%, effective, suggesting that other β1 integrin ligands upregulated in IAP-expressing cells, for instance collagen isoforms, cooperate in this response.

The ability of this autocrine/paracrine signaling circuit (Figure 8) to counter anoikis, likely provides an additional advantage for metastasis. Detachment of epithelial cells from the extracellular matrix (Frisch and Screaton, 2001), as well as unligation of so-called dependence receptors (Bredesen et al., 2005), is normally followed by apoptosis, but many tumor cell types manage to escape this response, and their ability to remain viable in suspension is thought to favor hematogenous or lymphatic dissemination (Nguyen and Massague, 2007). The requirements of transformed cells to counter anoikis have not been completely elucidated, and

a potential protective role of IAPs in this process, mostly XIAP, has been linked to caspase inhibition (Liu et al., 2006). At variance with this paradigm, IAP inhibition of anoikis did not involve release of survivin from mitochondria, which is required for cytoprotection (Dohi et al., 2007), but rather β1 integrin/fibronectin-mediated phosphorylation of FAK and Src kinases, thus similar to the paradigm of IAP-mediated tumor cell motility (Figure 8). This is in line with a protective role of these molecules against mitochondrial dysfunction during anoikis, potentially via activation of PI3 kinase/Akt-mediated cell survival (Bouchard et al., 2008). This pathway was selective for anoikis, as over-expression of survivin in transformed cells did not confer a further advantage for anchorage-independent cell growth, an observation consistent with the ability of activated FAK to attenuate oncogene-mediated colony formation in soft agar (Moissoglu and Gelman, 2003).

When tested in an in vivo model that recapitulates many of the steps of the metastatic process, unaffected by primary tumor growth, IAP signaling promoted rapid and extensive metastatic dissemination to the liver. Retrospective analysis of patient series identified IAPs, especially survivin, as contributors to tumor progression (Hinnis et al., 2007), but a role for these molecules as metastasis genes had not been previously postulated. Although metastasis of Ras-transformed fibroblasts has been recently linked to FAK dephosphorylation (Zheng et al., 2009), the IAP pathway of tumor cell dissemination occurred indistinguishably in tumor types with wild type or mutant Ras, and was associated with phosphorylation of FAK in metastatic foci in vivo. Importantly, the cytoprotective functions of survivin or XIAP were not required for IAP-mediated metastasis. Accordingly, over-expression of non-cytoprotective survivin in INS-1 cells (Dohi et al., 2007), or reconstitution of XIAP-deficient HCT116 cells with a D143A/W310A XIAP mutant that does not bind caspases (Lewis et al., 2004), mediated tumor cell invasion in vitro and promoted extensive liver metastasis in vivo. In addition, expression of anti-apoptotic Bcl-2 could not substitute for IAP signaling in metastasis, suggesting that suppression of cell death, alone, is insufficient to confer a successful metastatic phenotype in vivo. These data are consistent with previous observations that IAP activation of NFκB (Lu et al., 2007) is separable from its role in caspase inhibition (Lewis et al., 2004), and that metastatic dissemination in a transgenic model of melanoma does not require survivin cytoprotection (Thomas et al., 2007).

In summary, we identified IAPs as direct metastasis genes, orchestrating a cellular network of NFκB-dependent gene expression, β1 integrin signaling and activation of FAK and Src kinases required for metastatic dissemination (Figure 8). Although IAPs are not easily ‘drugable’ targets in cancer, molecular antagonists of both XIAP and survivin have been developed, and produced some encouraging patient responses in early-phase clinical trials (Altieri, 2008). The data presented here suggest that these agents may not have overlapping specificities, and could be differentially utilized as individualized therapeutic regimens in cancer patients. Accordingly, Smac mimetics XIAP antagonists may be predicted to activate apoptosis in tumors (Varfolomeev et al., 2007) but would not interfere with IAP signaling, which plays a pivotal role in tumor progression and metastasis (this study). Conversely, agents that directly suppress the levels of XIAP and survivin in tumors, including antisense molecules and transcriptional repressors of the survivin gene, which are also being tested in early phase clinical trials (Altieri, 2008), could be rationally tested as first-in-class anti-metastatic regimens in patients with advanced and metastatic disease.

EXPERIMENTAL PROCEDURES

Cell migration and invasion

Analysis of cell migration was carried out using 6.5-mm Transwell chambers (8- μm pore size; Costar). Inserts were prepared by coating the upper and lower surfaces with 15 μg/ml collagen (Cohesion, Palo Alto, CA) for 18 h at 4°C, followed by a blocking step with DMEM containing

0.25% heat-inactivated BSA for 1 h at 37°C. In some experiments, Transwell inserts were left uncoated. The various cell types were harvested, suspended in DMEM containing 0.25% heat-inactivated BSA, and added (1×10^5) to the upper chamber, with aliquots of conditioned medium collected from NIH3T3 fibroblasts placed in the lower chamber as chemoattractant. After 1 h incubation, non-migrating cells were removed mechanically from the upper chamber using a cotton swab. Cells migrated to the lower surface of the Transwell membrane were fixed in methanol for 10 min at 22°C, and membranes were mounted on glass slides using Vectashield mounting medium containing DAPI (Vector Laboratories, Burlingame, CA). Cell migration was quantified by counting the number of stained nuclei in five individual fields in each Transwell membrane, by fluorescence microscopy, in duplicate.

For analysis of cell invasion, the upper Transwell chamber (8- μm pore size; Costar) was coated with 0.5 μg Matrigel (Collaborative Research, Bedford, MA) diluted in cold water, and allowed to air dry. After 1 h incubation with DMEM, the various cell types (1×10^5) were added to the upper chamber for 6–24 h at 37°C. Cells that had invaded the lower surface of the membrane were fixed with methanol, stained with DAPI, and quantified by fluorescence microscopy. In some experiments, cells were incubated with the following pharmacologic inhibitors of Src (PP-2, 50 μM; SU6656, 25–50 μM), MEK (PD98059, 50 μM, or U0126, 25 μM), PI3 kinase (LY290042, 50 μM), or vehicle (DMSO) for 1 h at 37°C, added to Matrigel-coated membranes, and analyzed for cell invasion by fluorescence microscopy.

In vivo metastasis model

All experiments involving animals were approved by an Institutional Animal Care and Use Committee. Female SCID/beige mice (6–8 wk of age) were anesthetized with ketamine hydrochloride, the abdominal cavity was exposed by laparotomy, and animals were injected in the spleen with 2×10^6 MCF-7, MCF-7 SVV or MCF-7 SVV cells carrying stable shRNA knockdown of XIAP (MCF-7 SVV-XIAP KD) stably transfected with a luciferase cDNA. To avoid potential confounding effects on metastasis due to variable growth of a primary tumor, the spleen was removed 24 h after injection of the tumor cells. The incision was closed in two layers with vicryl 5/0 and wound clips. On d 1, 3, 7, and 11 after injection, animals were analyzed for metastatic disease by bioluminescence imaging using an IVIS-100 camera system for detection of luciferase expression (Xenogen, Alameda, CA). Briefly, mice were anesthetized with isoflurane and intraperitoneally injected with 2.2 mg luciferin sodium salt (GOLD Bio Technology, Inc) in PBS, pH 7.4. During image acquisition, isoflurane anesthesia was maintained using a nose cone delivery system. Both supine and prone images were scanned for a 3 min acquisition interval. Each image was acquired sequentially three to four times, and data were collected at the time of peak luminescence. The bioluminescence images were overlaid on black and white photographs of the mice collected at the same time. Signal intensity was quantified as the sum of all detected photon counts within a region of interest using Living image software (Xenogen, version 2.50). On d 11, all mice in the various groups were sacrificed and their livers were resected, and quantified for bioluminescence intensity, ex vivo. In some experiments, wild type ($XIAP^{+/+}$), $XIAP^{-/-}$ or $XIAP^{-/-}$ HCT116 cells stably transfected with D143A/W341A XIAP mutant (Lewis et al., 2004) lacking anti-apoptotic function (5 animals/group), were injected (5×10^6 cells) in the spleen of SCID/beige mice, followed by splenectomy as described above. Animals were sacrificed after 3 weeks, and livers were analyzed histologically. In other experiments, wild type INS-1 cells (4 animals), or INS-1 stably transfected with survivin (6 animals) that is not cytoprotective in this cell type (Dohi et al., 2007) or Bcl-2 (5 animals) were injected (5×10^6 cells) in the spleen of SCID/beige mice, followed by splenectomy 1 d after reconstitution. Mice were monitored for blood glucose content twice weekly, and sacrificed after 3 weeks for histologic examination of livers.

Histology

Livers from the various animal groups were fixed in buffered formalin, and embedded in paraffin. For insulin staining, sections were deparaffinized, rehydrated in water, and quenched for endogenous peroxidase. Epiope heat retrieval was carried out by steaming the slides in 10% sodium citrate for 20 min. Processed slides were rinsed in PBS, pH 7.4, and stained with an antibody to insulin using standard avidin-biotin-peroxidase technique (Histostain-plus, Zymed Laboratories). Slides were incubated with DAB as a chromogen and counterstained with hematoxylin. Control sections were processed as above with non binding IgG, and resulted in no detectable staining.

Statistical analysis

Data were analyzed using the unpaired t test on a GraphPad software package for Windows (Prism 4.0). A *p*-value of 0.05 was considered as statistically significant.

Supplementary Material

Refer to Web version on PubMed Central for supplementary material.

Acknowledgments

We thank Drs. Leslie Shaw for discussion, I.-S. Kim for a *fibronectin* promoter reporter construct, Michelle Kelliher for FSIPPW vector, Bert Vogelstein for HCT116 cells, Colin Duckett for XIAP$^{-/-}$ MEFs and D148A/W310A XIAP cDNA, and Robert Sherwin for INS-1 cells. This work was supported by National Institutes of Health grants CA89720 (LRL), CA107548 (AMM), CA78810, CA90917, CA118005 and HL54131 (DCA).

References

Altieri DC. Survivin, cancer networks and pathway-directed drug discovery. Nat Rev Cancer 2008;8:61–70. [PubMed: 18075512]

Birkey Reffey S, Wurthner JU, Parks WT, Roberts AB, Duckett CS. X-linked inhibitor of apoptosis protein functions as a cofactor in transforming growth factor-beta signaling. J Biol Chem 2001;276:26542–26549. [PubMed: 11356828]

Bittner M, Meltzer P, Chen Y, Jiang Y, Seftor E, Hendrix M, Radmacher M, Simon R, Yakhini Z, Ben-Dor A, et al. Molecular classification of cutaneous malignant melanoma by gene expression profiling. Nature 2000;406:536–540. [PubMed: 10952317]

Bouchard V, Harnois C, Demers MJ, Thibodeau S, Laquerre V, Gauthier R, Vezina A, Noel D, Fujita N, Tsuruo T, et al. B1 integrin/Fak/Src signaling in intestinal epithelial crypt cell survival: integration of complex regulatory mechanisms. Apoptosis 2008;13:531–542. [PubMed: 18322799]

Bredesen DE, Mehlen P, Rabizadeh S. Receptors that mediate cellular dependence. Cell Death Differ 2005;12:1031–1043. [PubMed: 16015380]

Clark EA, Golub TR, Lander ES, Hynes RO. Genomic analysis of metastasis reveals an essential role for RhoC. Nature 2000;406:532–535. [PubMed: 10952316]

Cory S, Adams JM. The Bcl2 family: regulators of the cellular life-or-death switch. Nat Rev Cancer 2002;2:647–656. [PubMed: 12209154]

Cukierman E, Pankov R, Yamada KM. Cell interactions with three-dimensional matrices. Curr Opin Cell Biol 2002;14:633–639. [PubMed: 12231360]

Dogan T, Harms GS, Hekman M, Karreman C, Oberoi TK, Alnemri ES, Rapp UR, Rajalingam K. X-linked and cellular IAPs modulate the stability of C-RAF kinase and cell motility. Nat Cell Biol 2008;10:1447–1455. [PubMed: 19011619]

Dohi T, Okada K, Xia F, Wilford CE, Samuel T, Welsh K, Marusawa H, Zou H, Armstrong R, Matsuzawa S, et al. An IAP-IAP complex inhibits apoptosis. J Biol Chem 2004;279:34087–34090. [PubMed: 15218035]

Dohi T, Xia F, Altieri DC. Compartmentalized phosphorylation of IAP by protein kinase A regulates cytoprotection. Mol Cell 2007;27:17–28. [PubMed: 17612487]

Fornaro M, Plescia J, Chheang S, Tallini G, Zhu YM, King M, Altieri DC, Languino LR. Fibronectin Protects Prostate Cancer Cells from Tumor Necrosis Factor-{alpha}-induced Apoptosis via the AKT/Survivin Pathway. J Biol Chem 2003;278:50402–50411. [PubMed: 14523021]

Frisch SM, Screaton RA. Anoikis mechanisms. Curr Opin Cell Biol 2001;13:555–562. [PubMed: 11544023]

Gaggioli C, Robert G, Bertolotto C, Bailet O, Abbe P, Spadafora A, Bahadoran P, Ortonne JP, Baron V, Ballotti R, Tartare-Deckert S. Tumor-derived fibronectin is involved in melanoma cell invasion and regulated by V600E B-Raf signaling pathway. J Invest Dermatol 2007;127:400–410. [PubMed: 16960555]

Geisbrecht ER, Montell DJ. A role for Drosophila IAP1-mediated caspase inhibition in Rac-dependent cell migration. Cell 2004;118:111–125. [PubMed: 15242648]

Ginsberg MH, Partridge A, Shattil SJ. Integrin regulation. Curr Opin Cell Biol 2005;17:509–516. [PubMed: 16099636]

Han S, Ritzenthaler JD, Sitaraman SV, Roman J. Fibronectin increases matrix metalloproteinase 9 expression through activation of c-Fos via extracellular-regulated kinase and phosphatidylinositol 3-kinase pathways in human lung carcinoma cells. J Biol Chem 2006;281:29614–29624. [PubMed: 16882662]

Helleman J, Jansen MP, Ruigrok-Ritstier K, van Staveren IL, Look MP, Meijer-van Gelder ME, Sieuwerts AM, Klijn JG, Sleijfer S, Foekens JA, Berns EM. Association of an extracellular matrix gene cluster with breast cancer prognosis and endocrine therapy response. Clin Cancer Res 2008;14:5555–5564. [PubMed: 18765548]

Hinnis AR, Luckett JC, Walker RA. Survivin is an independent predictor of short-term survival in poor prognostic breast cancer patients. Br J Cancer 2007;96:639–645. [PubMed: 17285125]

Hofer-Warbinek R, Schmid JA, Stehlik C, Binder BR, Lipp J, de Martin R. Activation of NF-kappa B by XIAP, the X chromosome-linked inhibitor of apoptosis, in endothelial cells involves TAK1. J Biol Chem 2000;275:22064–22068. [PubMed: 10807933]

Hughes PE, Renshaw MW, Pfaff M, Forsyth J, Keivens VM, Schwartz MA, Ginsberg MH. Suppression of integrin activation: a novel function of a Ras/Raf-initiated MAP kinase pathway. Cell 1997;88:521–530. [PubMed: 9038343]

Irie HY, Pearline RV, Grueneberg D, Hsia M, Ravichandran P, Kothari N, Natesan S, Brugge JS. Distinct roles of Akt1 and Akt2 in regulating cell migration and epithelial-mesenchymal transition. J Cell Biol 2005;171:1023–1034. [PubMed: 16365168]

Juliano RL, Reddig P, Alahari S, Edin M, Howe A, Aplin A. Integrin regulation of cell signalling and motility. Biochem Soc Trans 2004;32:443–446. [PubMed: 15157156]

Kaplan RN, Riba RD, Zacharoulis S, Bramley AH, Vincent L, Costa C, MacDonald DD, Jin DK, Shido K, Kerns SA, et al. VEGFR1-positive haematopoietic bone marrow progenitors initiate the pre-metastatic niche. Nature 2005;438:820–827. [PubMed: 16341007]

Lewis J, Burstein E, Reffey SB, Bratton SB, Roberts AB, Duckett CS. Uncoupling of the signaling and caspase-inhibitory properties of X-linked inhibitor of apoptosis. J Biol Chem 2004;279:9023–9029. [PubMed: 14701799]

Liu Z, Li H, Wu X, Yoo BH, Yan SR, Stadnyk AW, Sasazuki T, Shirasawa S, LaCasse EC, Korneluk RG, Rosen KV. Detachment-induced upregulation of XIAP and cIAP2 delays anoikis of intestinal epithelial cells. Oncogene 2006;25:7680–7690. [PubMed: 16799641]

Livant DL, Brabec RK, Kurachi K, Allen DL, Wu Y, Haaseth R, Andrews P, Ethier SP, Markwart S. The PHSRN sequence induces extracellular matrix invasion and accelerates wound healing in obese diabetic mice. J Clin Invest 2000;105:1537–1545. [PubMed: 10841512]

Lu M, Lin SC, Huang Y, Kang YJ, Rich R, Lo YC, Myszka D, Han J, Wu H. XIAP induces NF-kappaB activation via the BIR1/TAB1 interaction and BIR1 dimerization. Mol Cell 2007;26:689–702. [PubMed: 17560374]

Mehlen P, Puisieux A. Metastasis: a question of life or death. Nat Rev Cancer 2006;6:449–458. [PubMed: 16723991]

Mitra SK, Schlaepfer DD. Integrin-regulated FAK-Src signaling in normal and cancer cells. Curr Opin Cell Biol 2006;18:516–523. [PubMed: 16919435]

Moissoglu K, Gelman IH. v-Src Rescues Actin-based Cytoskeletal Architecture and Cell Motility and Induces Enhanced Anchorage Independence during Oncogenic Transformation of Focal Adhesion Kinase-null Fibroblasts. J Biol Chem 2003;278:47946–47959. [PubMed: 14500722]

Naugler WE, Karin M. NF-[kappa]B and cancer -- identifying targets and mechanisms. Current Opinion in Genetics & Development 2008;18:19–26. [PubMed: 18440219]

Nelson CM, Bissell MJ. Of extracellular matrix, scaffolds, and signaling: tissue architecture regulates development, homeostasis, and cancer. Annu Rev Cell Dev Biol 2006;22:287–309. [PubMed: 16824016]

Nguyen DX, Massague J. Genetic determinants of cancer metastasis. Nat Rev Genet 2007;8:341–352. [PubMed: 17440531]

Nobes CD, Hall A. Rho, rac, and cdc42 GTPases regulate the assembly of multimolecular focal complexes associated with actin stress fibers, lamellipodia, and filopodia. Cell 1995;81:53–62. [PubMed: 7536630]

Oshima K, Takeda M, Kuranaga E, Ueda R, Aigaki T, Miura M, Hayashi S. IKK epsilon regulates F actin assembly and interacts with Drosophila IAP1 in cellular morphogenesis. Curr Biol 2006;16:1531–1537. [PubMed: 16887350]

Parsons JT, Slack-Davis J, Tilghman R, Roberts WG. Focal adhesion kinase: targeting adhesion signaling pathways for therapeutic intervention. Clin Cancer Res 2008;14:627–632. [PubMed: 18245520]

Paszek MJ, Zahir N, Johnson KR, Lakins JN, Rozenberg GI, Gefen A, Reinhart-King CA, Margulies SS, Dembo M, Boettiger D, et al. Tensional homeostasis and the malignant phenotype. Cancer Cell 2005;8:241–254. [PubMed: 16169468]

Pohl C, Jentsch S. Final stages of cytokinesis and midbody ring formation are controlled by BRUCE. Cell 2008;132:832–845. [PubMed: 18329369]

Resch U, Schichl YM, Winsauer G, Gudi R, Prasad K, de Martin R. Siva1 is a XIAP-interacting protein that balances NF{kappa}B and JNK signalling to promote apoptosis. J Cell Sci. 2009

Salz W, Eisenberg D, Plescia J, Garlick DS, Weiss RM, Wu XR, Sun TT, Altieri DC. A survivin gene signature predicts aggressive tumor behavior. Cancer Res 2005;65:3531–3534. [PubMed: 15867343]

Sanna MG, Duckett CS, Richter BW, Thompson CB, Ulevitch RJ. Selective activation of JNK1 is necessary for the anti-apoptotic activity of hILP. Proc Natl Acad Sci U S A 1998;95:6015–6020. [PubMed: 9600909]

Scheel C, Onder T, Karnoub A, Weinberg RA. Adaptation versus selection: the origins of metastatic behavior. Cancer Res 2007;67:11476–11479. discussion 11479–11480. [PubMed: 18089773]

Sieg DJ, Hauck CR, Ilic D, Klingbeil CK, Schaefer E, Damsky CH, Schlaepfer DD. FAK integrates growth-factor and integrin signals to promote cell migration. Nat Cell Biol 2000;2:249–256. [PubMed: 10806474]

Slack JK, Catling AD, Eblen ST, Weber MJ, Parsons JT. c-Raf-mediated inhibition of epidermal growth factor-stimulated cell migration. J Biol Chem 1999;274:27177–27184. [PubMed: 10480934]

Srinivasula SM, Ashwell JD. IAPs: what's in a name? Mol Cell 2008;30:123–135. [PubMed: 18439892]

Stupack DG, Teitz T, Potter MD, Mikolon D, Houghton PJ, Kidd VJ, Lahti JM, Cheresh DA. Potentiation of neuroblastoma metastasis by loss of caspase-8. Nature 2006;439:95–99. [PubMed: 16397500]

Talmadge JE. Clonal selection of metastasis within the life history of a tumor. Cancer Res 2007;67:11471–11475. [PubMed: 18089772]

Thomas J, Liu T, Cotter MA, Florell SR, Robinette K, Hanks AN, Grossman D. Melanocyte expression of survivin promotes development and metastasis of UV-induced melanoma in HGF-transgenic mice. Cancer Res 2007;67:5172–5178. [PubMed: 17545596]

Varfolomeev E, Blankenship JW, Wayson SM, Fedorova AV, Kayagaki N, Garg P, Zobel K, Dynek JN, Elliott LO, Wallweber HJ, et al. IAP antagonists induce autoubiquitination of c-IAPs, NF-kappaB activation, and TNFalpha-dependent apoptosis. Cell 2007;131:669–681. [PubMed: 18022362]

Weigelt B, Peterse JL, van 't Veer LJ. Breast cancer metastasis: markers and models. Nat Rev Cancer 2005;5:591–602. [PubMed: 16056258]

Williams CM, Engler AJ, Slone RD, Galante LL, Schwarzbauer JE. Fibronectin expression modulates mammary epithelial cell proliferation during acinar differentiation. Cancer Res 2008;68:3185–3192. [PubMed: 18451144]

Yao ES, Zhang H, Chen YY, Lee B, Chew K, Moore D, Park C. Increased {beta}1 Integrin Is Associated with Decreased Survival in Invasive Breast Cancer. Cancer Res 2007;67:659–664. [PubMed: 17234776]

Yeatman TJ. A renaissance for SRC. Nat Rev Cancer 2004;4:470–480. [PubMed: 15170449]

Zheng Y, Xia Y, Hawke D, Halle M, Tremblay ML, Gao X, Zhou XZ, Aldape K, Cobb MH, Xie K, et al. FAK phosphorylation by ERK primes ras-induced tyrosine dephosphorylation of FAK mediated by PIN1 and PTP-PEST. Mol Cell 2009;35:11–25. [PubMed: 19595712]

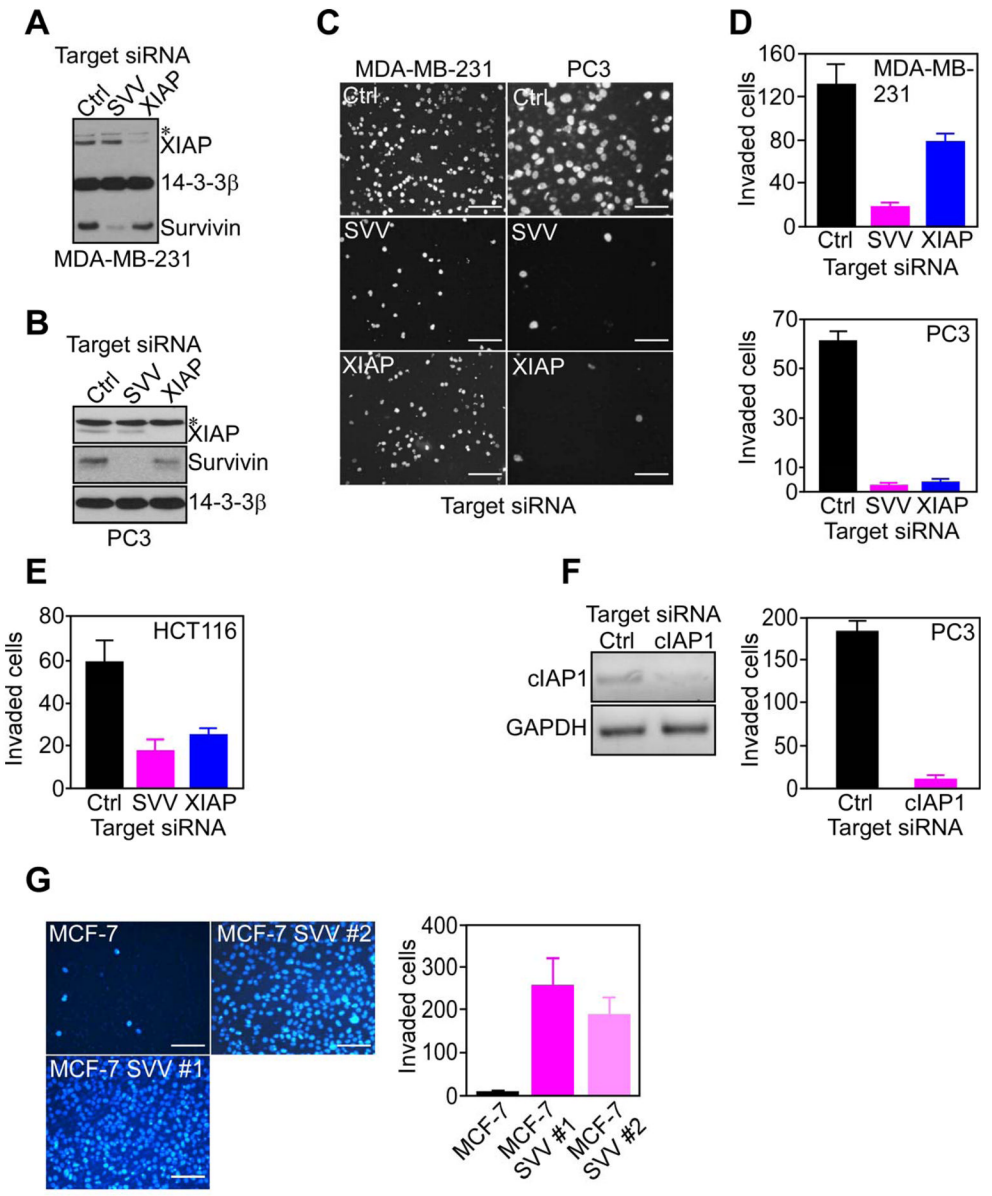

Figure 1. IAP-mediated tumor cell invasion

(A, B) Breast adenocarcinoma MDA-MB-231 (A) or prostate adenocarcinoma PC3 (B) cells transfected with control (Ctrl) or survivin (SVV)- or XIAP-directed siRNA, were analyzed by Western blotting after 48 h. *, non-specific. (C–E) The indicated siRNA transfected cell types were analyzed for invasion through Matrigel-coated Transwell inserts after 6 h by DAPI staining (C), and quantified (D). Scale bars, 200 μm (MDA-MB-231), 100 μm (PC3). (F) PC3 cells were transfected with control (Ctrl) or cIAP1-directed siRNA, and analyzed by PCR (*left*) and Matrigel invasion after 6 h (*right*). (G) MCF-7 or MCF-7 SVV cells (clones #1 and #2) were analyzed for Matrigel invasion after 6 h by DAPI staining (*left*), and quantified (*right*). Scale bars, 200 μm. For panels D–G data are the mean±SD of duplicates of a representative experiment out of at least two independent determinations. See also Figure S1.

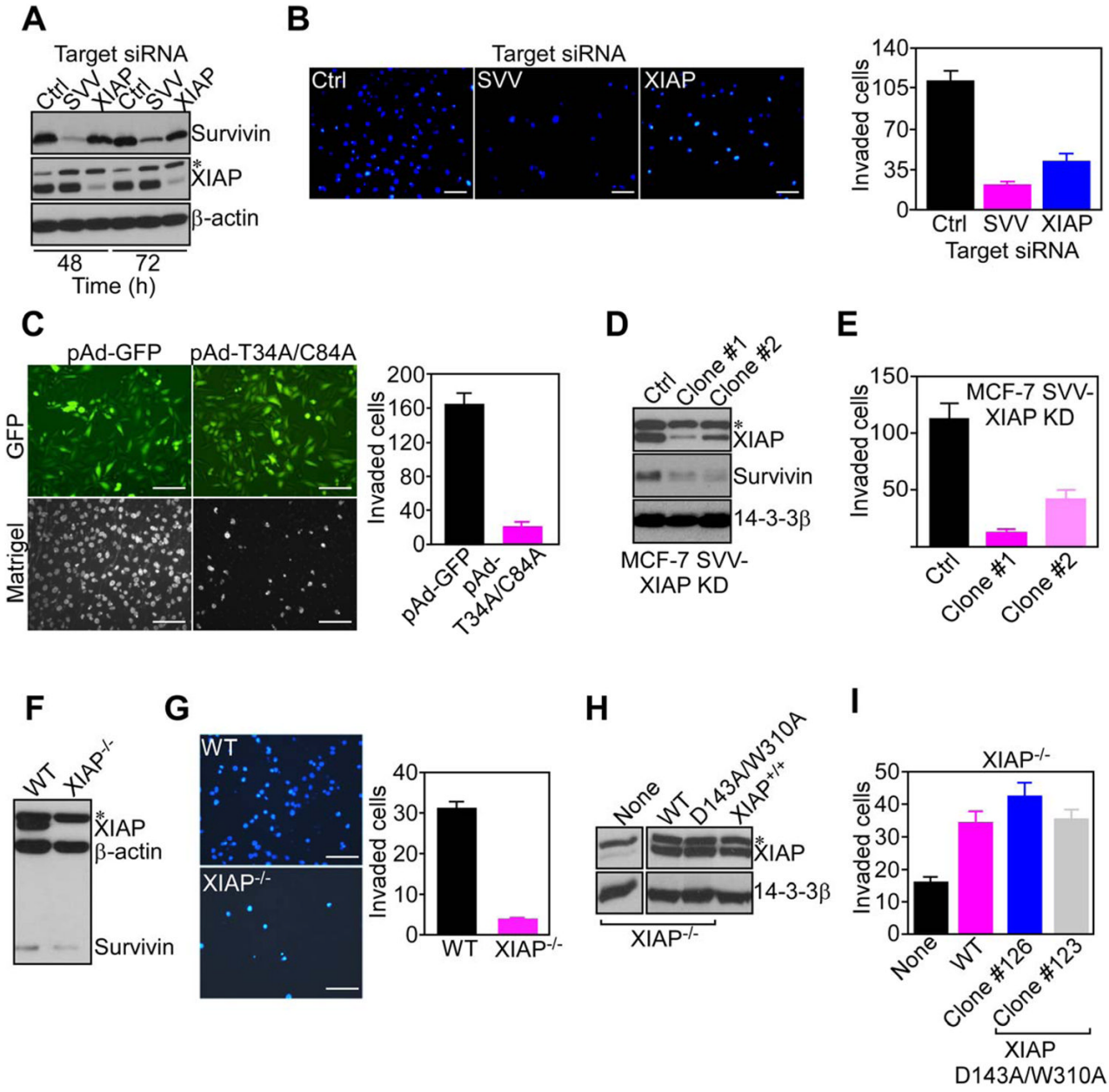

Figure 2. IAP targeting inhibits tumor cell invasion

(A) MCF-7 SVV cells transfected with control (Ctrl) or survivin (SVV)- or XIAP-directed siRNA were analyzed by Western blotting. (B) MCF-7 SVV cells (clone #1) transfected with the indicated siRNA were analyzed for Matrigel invasion after 6 h by DAPI staining (*left*), and quantified (*right*). Scale bars, 200 μm. (C) MCF-7 SVV cells were transduced with pAd-GFP or pAd-T34A/C84A survivin mutant, and imaged after 24 h for GFP expression (*top*), or DAPI staining of Matrigel invasion (*bottom*). Invaded cells were quantified after 6 h (*right*). Scale bars, 200 μm. (D, E) MCF-7 SVV cells with stable shRNA knockdown of XIAP (MCF-7 SVV-XIAP KD; clones #1 and #2) were analyzed by Western blotting (D), and quantified for Matrigel invasion after 6 h (E). (F, G) Wild type (WT) or XIAP$^{-/-}$ HCT116 cells were analyzed by Western blotting (F), and characterized for Matrigel invasion after 6 h by DAPI staining (G, *left*), and quantified (G, *right*). Scale bars, 200 μm. (H) XIAP$^{-/-}$ HCT116 cells were stably

transfected with WT XIAP or D143A/W310A XIAP mutant, and analyzed by Western blotting. Wild type ($XIAP^{+/+}$) HCT116 cells were used as a control. (I) $XIAP^{-/-}$ HCT116 cells stably expressing WT XIAP or XIAP D143A/W310A mutant (clones #123 and #126) were quantified for Matrigel invasion after 6 h by DAPI staining. For panels B, C, E, G, I, data are the mean ±SD of duplicates of a representative experiment out of at least two independent determinations. See also Figure S2.

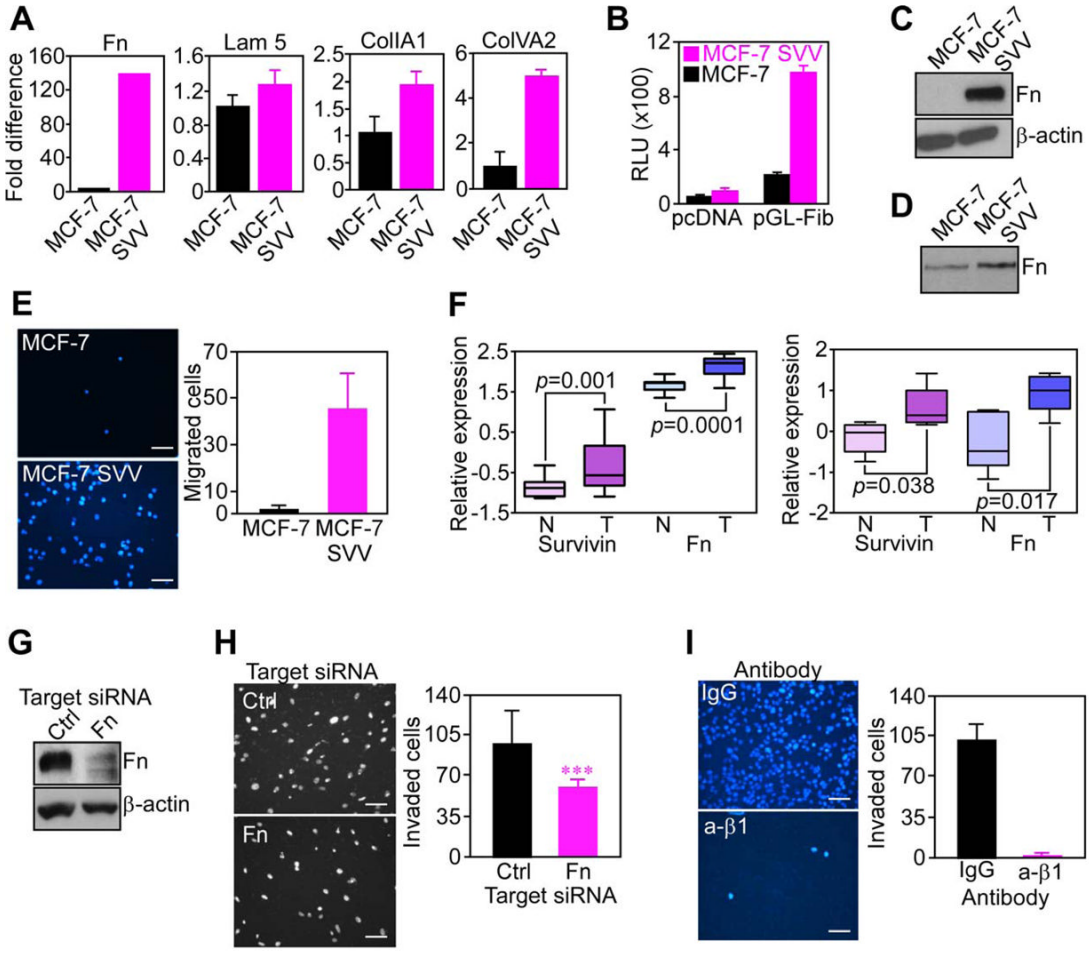

Figure 3. IAP induction of fibronectin

(A) RNA was amplified for the indicated gene products, and normalized to GAPDH expression. Fn, fibronectin; Lam 5, laminin 5; CollA1, collagen A1; Col IVA2, collagen IV A2. (B) Cells transfected with pcDNA or a 1.9 kb *fibronectin* promoter-luciferase construct (pGL-Fib) were analyzed after 24 h for β-galactosidase-normalized luciferase activity. RLU, relative luciferase units. (C) Cell extracts were analyzed by Western blotting. (D) Conditioned media collected after 48 h was normalized per cell number and analyzed by Western blotting. (E) Cell migration on uncoated Transwell inserts was analyzed by DAPI staining (*left*), and quantified (*right*). Scale bars, 200 μm. (F) Microarray datasets of two breast cancer patient series were analyzed for expression of survivin and fibronectin (Fn) in tumor (T) *versus* normal (N) tissues. (G) MCF-7 SVV cells transfected with control (Ctrl) or fibronectin (Fn)-directed siRNA were analyzed after 48 h by Western blotting. Scale bars, 200 μm. (H) siRNA-transfected cells as in G were analyzed for Matrigel invasion after 6 h by DAPI staining (*left*), and quantified (*right*). Scale bars, 200 μm. ***, p=0.0006. (I) MCF-7 SVV cells were incubated with non-binding IgG or a function-blocking antibody to β1 integrin (β1), and characterized for Matrigel invasion after 6 h by DAPI staining (*left*), and quantified (*right*). Scale bars, 200 μm. For panels A, B, E, H, I, data are the mean±SD of duplicates of a representative experiment out of at least two independent determinations. For panel F, data are shown as box plots, where whiskers are the minimum and maximum, and the box is the upper and lower quartile. See also Figure S3.

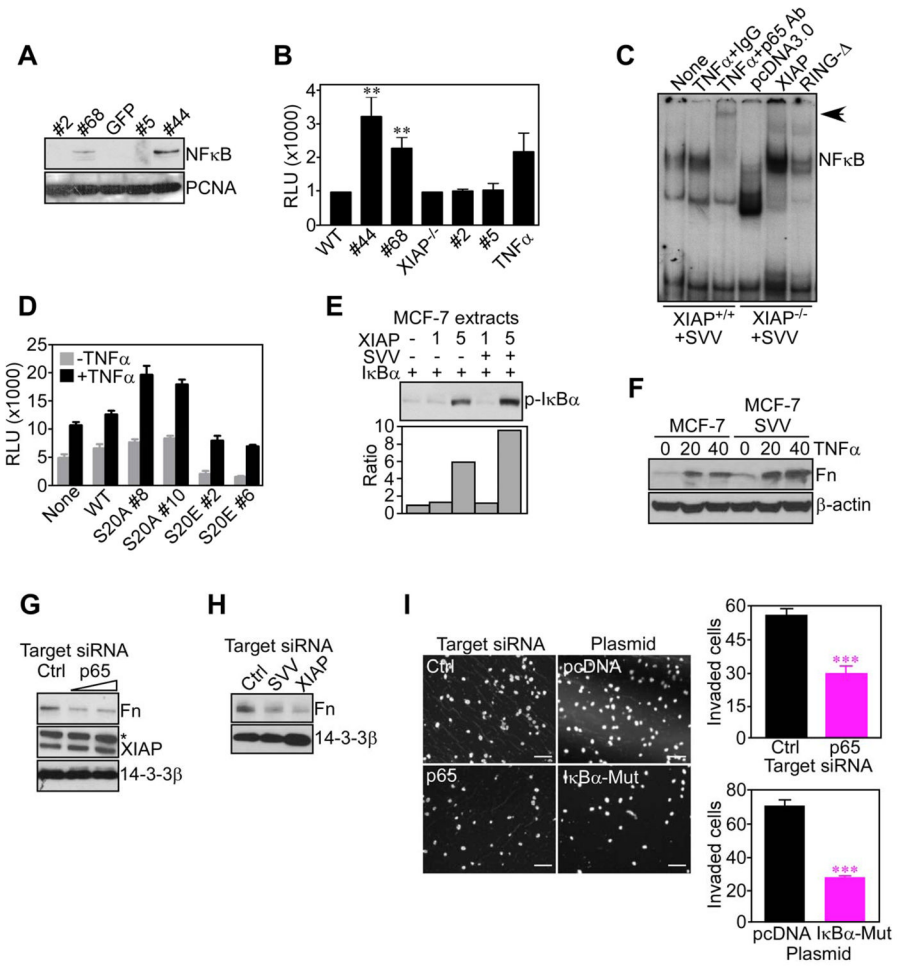

Figure 4. NFκB induction of fibronectin mediates IAP tumor cell invasion

(A) Nuclear extracts from WT (clones #44 and #68) or XIAP$^{-/-}$ (clones #2 and #5) MEF stably transfected with survivin were analyzed by Western blotting. (B) Survivin-expressing WT or XIAP$^{-/-}$ clones as in (A) were analyzed for β-galactosidase-normalized NFκB-luciferase reporter activity. TNFα-stimulated cells were used as a control. **, p=0.006. (C) Nuclear extracts from WT or XIAP$^{-/-}$ clones expressing survivin as in (A) were incubated with a ^{32}P-labeled NFκB probe in the presence of IgG or an antibody to p65 NFκB, followed by autoradiography. In reconstitution experiments, XIAP$^{-/-}$ cells were transfected with wild type XIAP or RING-less XIAP (RING-Δ). (D) INS-1 clones stably transfected with the indicated survivin mutant were analyzed for β-galactosidase-normalized NFκB luciferase promoter activity, with or without TNFα. For panels B and E, RLU, relative luciferase units. (E) Extracts from MCF-7 cells incubated with recombinant survivin (SVV), XIAP, or IκBα were analyzed by Western blotting. *Bottom*, densitometric quantification of protein bands. (F) Unstimulated or TNFα (ng/ml)-stimulated cells were analyzed by Western blotting. (G) MCF-7 SVV cells transfected with control (Ctrl) or p65 NFκB-directed siRNA were analyzed after 48 h by Western blotting. *, non-specific. (H) MCF-7 SVV cells transfected with control (Ctrl), survivin (SVV)- or XIAP-directed siRNA were analyzed by Western blotting. (I) MCF-7 SVV cells transfected with control (Ctrl) or p65 NFκB-directed siRNA, or, alternatively, pcDNA or IκBα mutant (IκBα-Mut), were analyzed for Matrigel invasion after 6 h by DAPI staining (*left*), and quantified (*right*). Scale bars, 200 μm. ***, p<0.0001. Mean±SD of duplicates of a

representative experiment out of at least two independent determinations. For panels B, D, data are the mean±SEM of triplicates of two independent determinations. See also Figure S4.

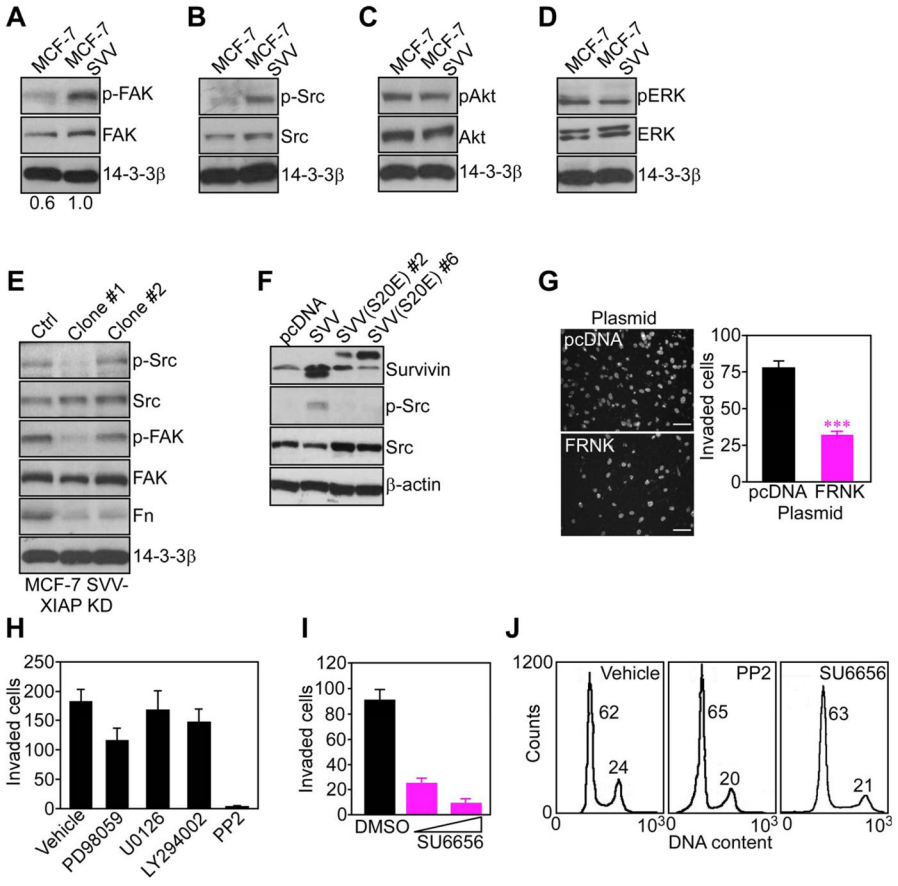

Figure 5. IAP activation of cell motility kinases

(A-D) Adherent cells were analyzed after 48 h by Western blotting for phosphorylation/expression of FAK (A), Src (B), Akt (C), or ERK1,2 (D). (E) MCF-7 SVV cells with stable shRNA knockdown of XIAP (MCF-7 SVV-XIAP KD; clones #1 and #2) were analyzed by Western blotting. (F) INS-1 cells stably transfected with wild type survivin (SVV) or survivin S20E mutant (clones #2 and #6) were analyzed by Western blotting. (G) MCF-7 SVV cells transfected with pcDNA or FAK dominant negative FRNK mutant were analyzed for Matrigel invasion after 6 h by DAPI staining (*left*), and quantified (*right*). Scale bars, 200 μm. ***, $p<0.0001$. (H) MCF-7 SVV cells treated with the indicated pharmacologic inhibitors were quantified for Matrigel invasion after 6 h. (I) MCF-7 SVV cells treated with the Src inhibitor SU6656 (25–50 μM) were quantified for Matrigel invasion after 6 h. (J) MCF-7 SVV cells were incubated with vehicle (DMSO) or the indicated Src inhibitors, and analyzed for DNA content after 24 h by propidium iodide staining and flow cytometry. The percentage of cells in the G1 or G2/M phase of the cell cycle is indicated. For panels G, H, I, data are the mean ±SD of duplicates of a representative experiment out of at least two independent determinations. See also Figure S5.

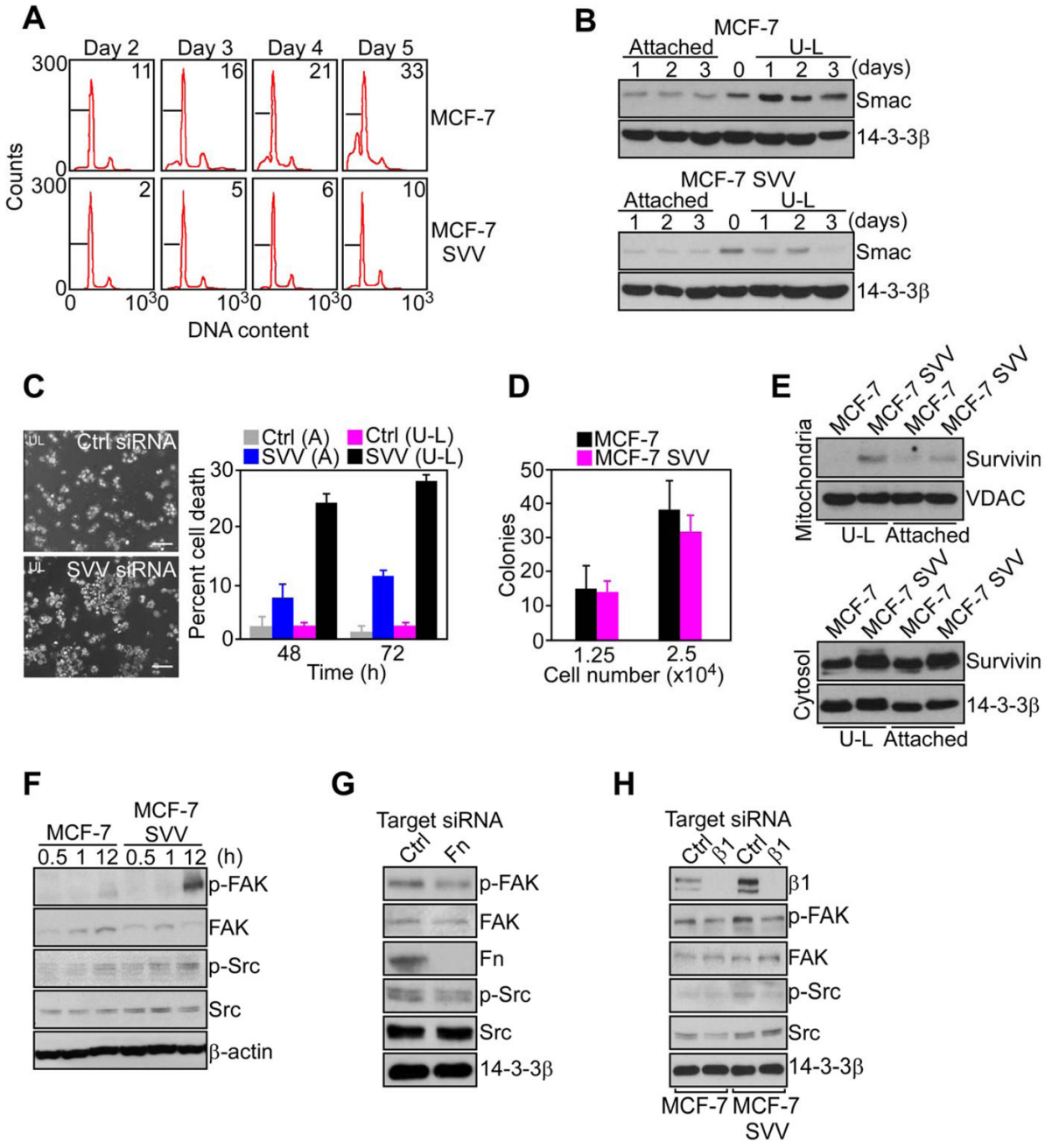

Figure 6. IAP suppression of anoikis

(A) Cells were maintained in suspension using ultra-low (*U-L*) attachment plates, and analyzed at the indicated time intervals by propidium iodide staining and flow cytometry. The percentage of cells with hypodiploid (apoptotic) DNA content is indicated. (B) Cytosolic extracts of cultures maintained attached or in suspension (*U-L*) were analyzed by Western blotting. (C) Cultures maintained attached (*A*) or in suspension (*U-L*) were transfected with control (Ctrl) or survivin (SVV)-directed siRNA, and analyzed by phase contrast microscopy (*left*) and quantified for nuclear morphology of apoptosis after 48 h (*right*). Scale bars, 200 μm. (D) Cells were plated at the indicated numbers in semi-solid medium, and colonies were scored after 2 weeks by light microscopy. (E) Mitochondria (*top*) or cytosolic (*bottom*) extracts of cultures attached or in suspension (*U-L*) were analyzed by Western blotting. (F) Cultures in suspension

were analyzed by Western blotting. (G) MCF-7 SVV cells transfected with control (Ctrl) or fibronectin (Fn)-directed siRNA in suspension were analyzed by Western blotting. (H) Cells transfected with control (Ctrl) or β1 integrin (β1)-directed siRNA were analyzed by Western blotting. For panels C, D, data are the mean±SD of duplicates of a representative experiment out of at least two independent determinations. See also Figure S6.

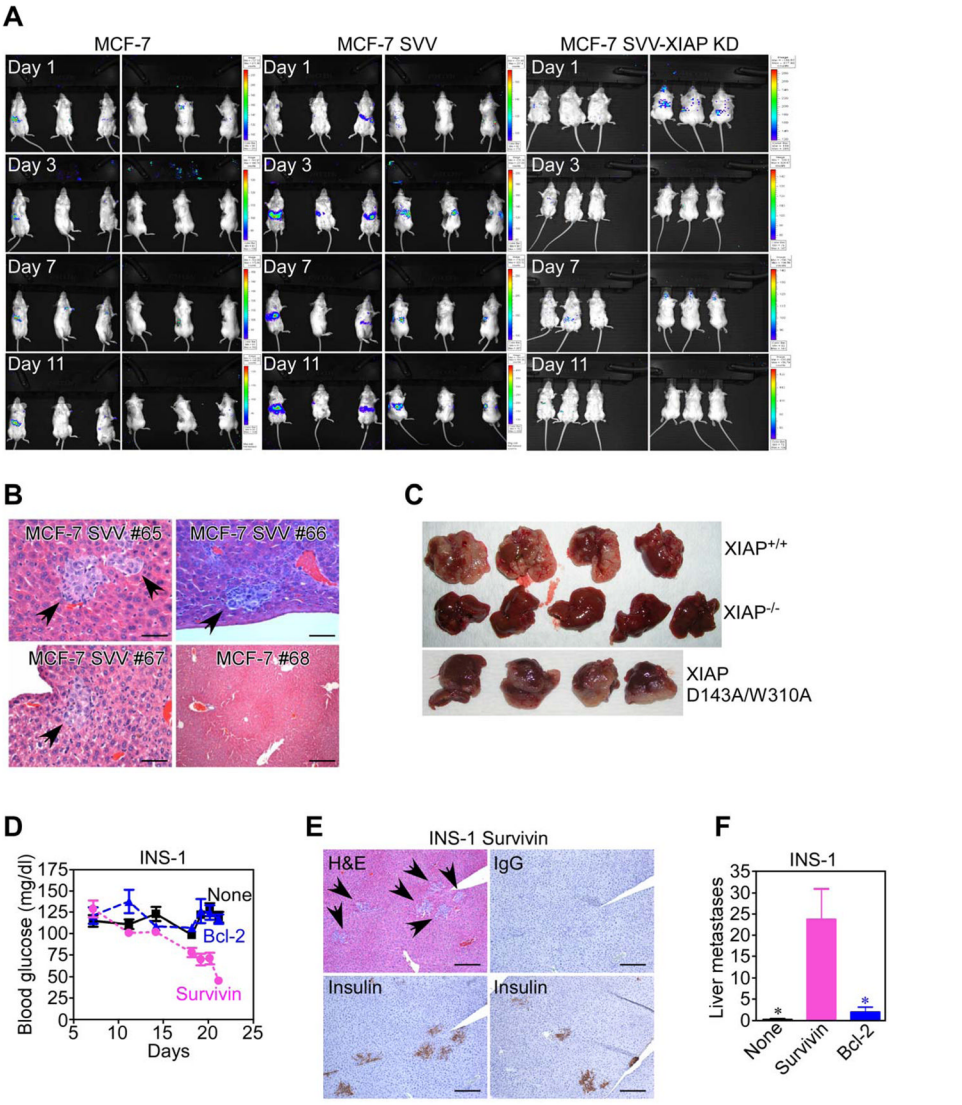

Figure 7. IAP-mediated metastasis, <u>in vivo</u>

(A) MCF-7, MCF-7 SVV or MCF-7 SVV cells carrying stable knockdown of XIAP (MCF-7 SVV-XIAP KD) stably transfected with luciferase were injected in the spleen of SCID/beige mice, and analyzed for metastatic tumor growth at the indicated time intervals, by bioluminescence imaging. (B) Livers from representative animals (#) reconstituted as indicated were harvested at d. 11, and analyzed by hematoxylin-eosin (H&E) staining and light microscopy. *Arrows*, metastatic foci. Scale bars, 100 μm, 500 μm. (C) $XIAP^{+/+}$, $XIAP^{-/-}$ or XIAP D143A/W310A mutant HCT116 cells were injected in the spleen of SCID/beige mice, and resected livers were examined macroscopically after 2 weeks. (D) SCID/beige mice reconstituted with INS-1 cells stably transfected with survivin or Bcl-2 were analyzed for blood glucose levels. (E) Livers of animals reconstituted with INS-1 cells transfected with survivin were stained by H&E or insulin. IgG, non binding antibody. *Arrows*, metastatic foci. Scale bars, 500 μm. (F) Metastatic foci of INS-1 cells were counted blindly in four independent microscopy fields of serial liver sections harvested from the indicated animal groups. *, p=0.017–0.025. For panels D, F, data are the mean±SEM. See also Figure S7.

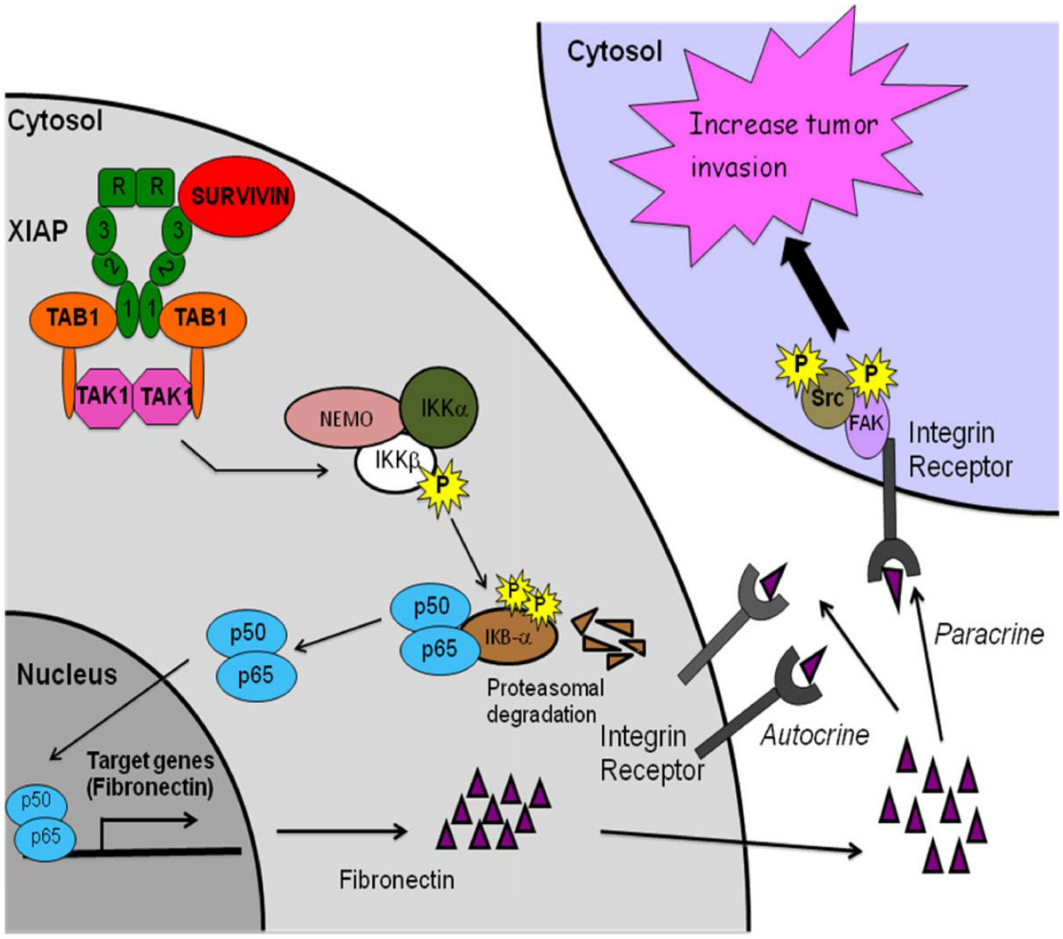

Figure 8. Schematic mechanistic model of IAP-induced metastasis
See text for details.